11th International Workshop on Ship and Marine Hydrodynamics
Hamburg, Germany, September 22-25, 2019

SPIV Measurement for a Self-propelled Ship in Regular Head Waves with Different Amplitudes

Benson O. Mwangi*, Haruki Nango, Yasuyuki Toda

Osaka University, Department of Naval Architecture and Ocean Engineering
2-1 Yamadaoka, Suita, Osaka 565-0871, Japan

*Corresponding author, benson_mwangi@naoe.eng.osaka-u.ac.jp

ABSTRACT

In this study, the wave amplitude dependency on a ship advancing in regular head waves with different amplitudes is investigated by Experimental Fluid Dynamics (EFD) method. The thrust, towing force and 3DOF (Degree of Freedom) motions as well as the flow field around the stern of KVLCC2 (KRISO Very Large Crude-oil Carrier2) tanker model advancing at design Froude number, Fr=0.142 are measured. Three wavelengths; λ/L=1.1, 1.6 and 2 are selected and for each wavelength five different wave amplitudes; A=0.75, 1.5, 3, 4 and 4.3 cm are used. The motions and force measurement was done for with and without propeller conditions whereas the SPIV (Stereo-Particle Image Velocimetry) measurement was done for without propeller condition.

The motions and force measurement results were analyzed by Fourier series expansion and the data was reconstructed by ignoring the higher harmonics than 7th harmonics to understand the fluctuation shape in one period. It was noted that the 1st, 2nd and 3rd harmonic components are responsible for the thrust oscillations with a quickly increasing slope and a slowly decreasing slope. For motions, the 1st harmonic components were enough to obtain the original motion trend. The 1st harmonic values for heave and pitch motions increase linearly with increase in wave amplitude. On the other hand, the thrust mean values decrease slightly with increase in wave amplitude. For the PIV results, the vertical relative motion between the propeller disk and the low velocity region, due to bilge vortices, was observed. As the wave amplitude increases this relative motion increases and high velocity flow enters the propeller plane from the bottom.

In conclusion, the velocity distribution around the stern was analysed and discussed with respect to the thrust fluctuation in waves. The trend could be explained although the velocity field was measured for without propeller condition.

1 INTRODUCTION

To curb the production of greenhouse gas (GHG) emissions from the shipping industry, there is need to improve the propulsive performance, including the engine characteristics, for ships in waves. However, the fundamental understanding of the propeller-hull interaction for ships in waves is insufficient because the viscous inflow velocity into the propeller plane in waves has not been done sufficiently partly due to the level of difficulty in conducting experiments. This notwithstanding, studies on propulsion, resistance and flow field around ships in waves have been done by several researchers by using EFD and CFD (Computational Fluid Dynamics) methods.

For example, Nakamura and Naito [1] studied the resistance and self-propulsion for a single screw high-speed container ship in regular and irregular waves. The inflow velocity into the propeller disk was measured using a ring-type wake meter in regular head waves. It was concluded that the time averaged mean values of effective wake are larger in waves than in still water due to the effect of ship motions, and that the fluctuations

of the propeller thrust and torque are mainly due to the fluctuation of the axial inflow velocity into the propeller disk.

Tsukada et al [2] conducted an experiment in regular head waves with λ/L=0.5 and 1 in which a ship was towed both in heave and pitch free condition, and motion fixed. The result for wake fraction and mean circulation in one encounter period was shown, and it was concluded that the nominal wake increases in regular waves especially in longer waves where the vertical ship motions are large. Calcagno et al [3] carried out an experimental investigation of a five blade MAU propeller wake behind a Series 60 C_B=0.6 ship model by stereo PIV in a large free surface cavitation tunnel. They identified and discussed the blade viscous wake, the trailing vortex sheets and velocity fluctuation distributions. They also described the complex interaction between the hull wake and the propeller through the evolution of the mean velocity components and the vorticity fields. Ohashi et al [4] used CFD-SURF to do unsteady RANS simulations of flows around KVLCC2 tanker model ship with motions in regular waves. In their study, vortices were observed in the propeller plane for long wavelengths and this was attributed to ship motions. It was also noted that the increase in time averaged nominal wake coefficient is as a result of the interaction between the waves and ship motions.

Sadat-Hosseini et al [5] studied the wake fields for KVLCC2 at Fr=0.142 and 0.25 for short and long, regular waves (λ/L=0.6, 1.1 and 1.6) at wave amplitude of 3cm using URANS (Unsteady Reynolds-Averaged Navier-Stokes) simulations and validated the results against EFD. The results show that the wake fields are compressed by higher velocity from the outer flow in both y and z directions when the ship aft is located on the crest and they are expanded when in the wave trough. A study on the added resistance, motions and wake fields at the propeller plane of KVLCC2 tanker model in fully-loaded and ballast conditions in head waves was conducted by Wu [6] using CFDShip-Iowa V4.5. The bilge vortex shedding from the hull body into the propeller plane and a secondary vortex induced by the vertical stern motion and shedding around the shaft were observed. Furthermore, it was observed that when the ship moves down there are counter-rotating vortices above the shaft and the boundary layer gets thicker in this region.

Kim et al [7] measured the velocity field near the propeller using SPIV system in order to investigate the effect of waves and ship motions to the propeller inflow velocity distribution. It was concluded that the orbital motion has an effect on the velocity distribution at the propeller plane, and that the low velocity region, due to bilge vortices, moves vertically relative to the propeller disk. Wu et al [8] carried out a detailed analysis on the wake field for KVLCC2 tanker model in ballast condition using URANS and results validated against experimental result. It was established that the bilge vortex moves relative to the ship stern motion and the low speed area with a secondary vortex induced by the dummy hub movement. Moreover, the wake field becomes narrower or wider due to the higher or lower orbital velocity.

Tokgoz et al [9] used CFDShip-Iowa V4.5 and SPIV system to measure the flow field around a self-propelled KVLCC2 tanker ship model at Fr=0.142 in regular head waves of λ/L=0.6, 1.1 and 1.6 at wave amplitude of 3cm. The ship wake behaviour was analysed in detail and its effect on the propeller performance investigated, and it was revealed that in long waves (λ/L=1.1 and 1.6) thrust oscillates with higher harmonic components. It was also observed that the increasing and decreasing thrust slopes were clearly different especially for longer waves as compared to short waves, and this was attributed to the movement of the bilge vortices relative to the ship motions and pressure gradient between the inner and outer boundary layers.

Recently, Hossain et al [10] studied the wake flow field at the propeller plane for a 3.2m KRISO Container Ship (KCS) model in regular head waves using CFDShip-Iowa V4.5 and SPIV. In one period, the bilge vortices were observed at the side or above the dummy propeller boss unlike in KVLCC2 in which the bilge vortex moves even outside the propeller radius. This was attributed to the fine shape of KCS at the stern with almost a T shaped wide transom and hence low mass at the stern.

In summary, from the study of Tokgoz et al [9] the relation between thrust time history and flow field is discussed, and it is noted that the vertical relative motion between the propeller disk and the bilge vortices is very important to explain the thrust fluctuation. So, it seems that the wave amplitude has a lot of effect on the thrust fluctuation and the averaged wake. Therefore, in this study, the flow field around the stern of KVLCC2 model ship in regular head waves with different amplitudes is measured using the SPIV system as well as thrust, torque, towing force and 3DOF motion to investigate how the velocity distribution changes with the wave amplitude and its effect on the amount of thrust delivered by the propeller.

2 TEST CONDITIONS

The design Froude number, Fr is 0.142 (0.795m/s). Two experiments were done (1st one during winter and 2nd one in spring), and the Reynold numbers were $Re = 1.908 \times 10^6$ and $Re = 2.258 \times 10^6$ for the 1st

and 2nd experiments respectively. Wave conditions were three long waves of λ/L=1.1, 1.6 and 2, and for each wavelength five wave amplitudes were done. The summary of the test conditions for the experiments is as shown in Table 1 in which A is wave amplitude and L is the ship length between perpendiculars.

Table 1: Test conditions.

λ/L	A(cm)	A/L
1.1	0.75	0.00234375
	1.5	0.0046875
1.6	3	0.009375
2	4	0.0125
	4.3	0.0134375

3 EXPERIMENTS

The motions and force measurement experiment was done separately from the SPIV measurement. A fully-loaded 3.2m KVLCC2 tanker model was used and its particulars are stated by Wu et al [8]. The ship model and coordinate system used in both experiments are as shown in Figure 1. The positive x was in the direction of flow, y and z were positive in the starboard and upwards directions respectively. For the self-propulsion experiment, a 4-blade, 0.0986m diameter MOERI propeller model (right handed) was used.

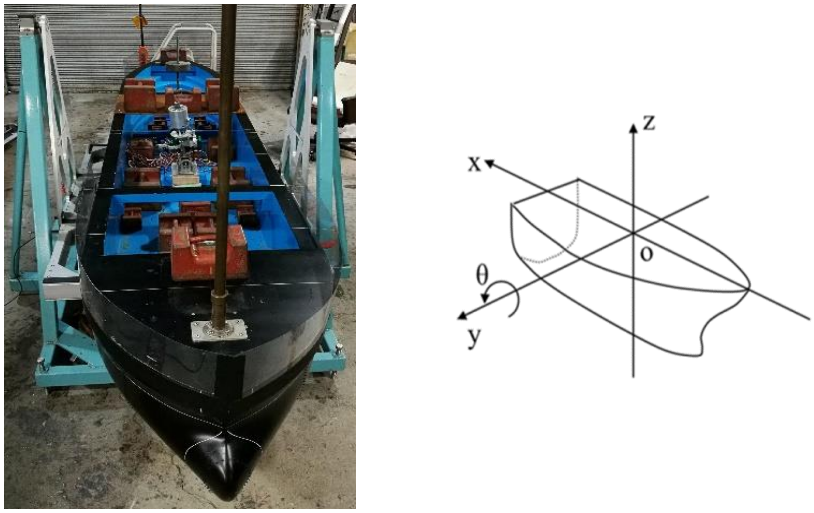

Figure 1: KVLCC2 Tanker model and coordinate system.

3.1 Motions and Force Measurement

A pitch-free gimbal and heaving rod were fixed on the CG (Center of Gravity) of the ship for pitch and heave free motions, and a yaw guide was fitted at the bow part to constrain the ship from yaw motion. The ship model was towed via a light weight carriage connected to the main carriage by a weak spring for surge free motion. An external force, F_0 was applied to prevent the weak spring from overstretching. The weak spring and the constant external force were mimicked by a servo-motor in this experiment and the force is adjusted by preliminary tests so as to keep the mean surge motion at zero. For self-propulsion tests, different propeller speeds, as determined from preliminary tests of previous experiments, were used; for λ/L=1.1, 21 rps (revolutions per second) whereas for λ/L=1.6 and 2, 15.89 rps were used.

Incident wave data were collected at the servo-type wave height meter which was mounted on the carriage, 3.52m upstream of the ship FP (Forward perpendicular). The ship motion was 3DOF (free to heave, pitch and surge). These motions were measured by potentiometers. In the self-propulsion experiment, thrust

and torque were measured by a motor-driven dynamometer which was connected to the propeller by a shaft. The schematic diagram of the experimental set up is as shown in Figure 2 (a).

3.2 SPIV Measurement

The underwater SPIV system was used to measure the flow field at the ship AP (After Perpendicular). For larger wave amplitudes, the SPIV measurement was done in two vertical positions with an overlap so as to capture the whole flow field. The target measurement station was the propeller plane but because of a lot of laser reflections from the dummy hub, the measurement plane was shifted to the AP. The measurement at AP could give a good result as well because from the boundary layer approximation, the flow field at the propeller plane and AP is similar.

The wave height meter was installed 3.314m upstream of the ship FP and this is where the phases for the PIV measurement were set. It is equipped with a probe which is controlled by a servo-motor and it moves with the wave surface. Hence, the wave elevation data is recorded and sent as a pulse signal to the data collecting computer. The same signal is sent to the PIV system via the PTU (programmable timing unit), which adjusts the delay time, for image recording. This is achieved by a program code in the computer that is connected to the wave height meter to act as a phase synchronizer. The wave encounter period is input into the program code and by this, the PIV measurement was done at all the planned phases (0, 90, 180 and 270). The zero phase is the zero crossing up of the incident wave.

The PIV system components used include two CCD (charge-coupled device) cameras, 135 mJ double-pulsed Nd YAG laser and optic system for light sheet generation, a computer with Davis (data acquisition and visualization) software for acquisition and processing of images. The details about the PIV system components are discussed by Kim [7]. The SPIV measurement experimental set up is as shown in Figure 2 (b), and the red box shows the wave height meter.

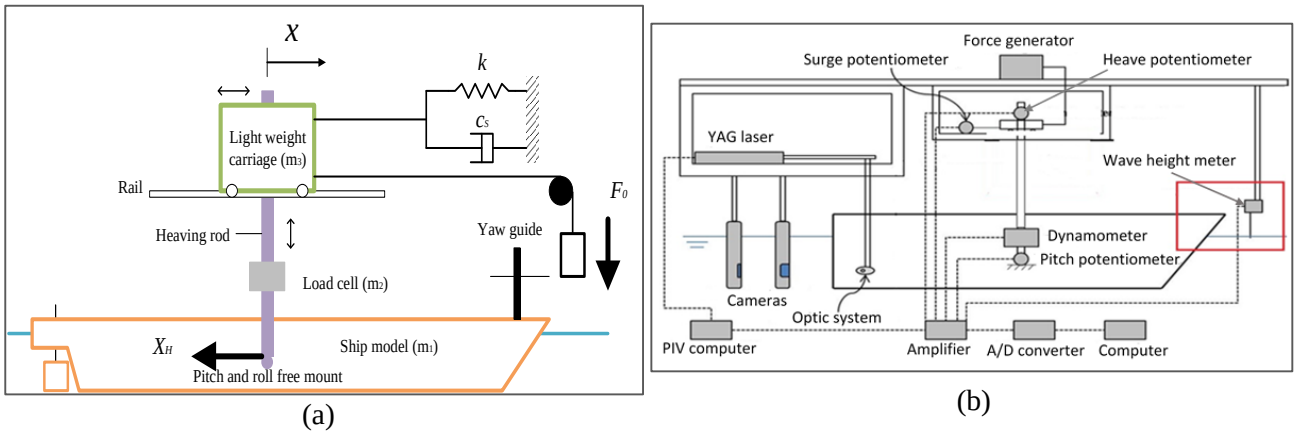

Figure 2: (a) The Motions and force (b) SPIV measurement experimental set ups.

4 RESULTS

4.1 Motions and Force Measurement Result

In this experiment, the wave elevation, x-force, heave, pitch and surge were measured both in calm water and in waves whereas thrust and torque were measured in waves only.

These results were analysed by Fourier series expansion using equations 4.1 ~ 4.4, and the data was reconstructed by ignoring higher harmonics than 7th harmonics so as to understand the fluctuation shape in one period. So, for thrust and torque a lot of noise due to vibration of the connection joint between the motor and the self-propulsion dynamometer was eliminated. From the Fourier series analysis, it was noted that the 1st, 2nd and 3rd harmonic components are responsible for the thrust oscillations with a quickly increasing slope and slowly decreasing slope. For motions, it was found out that the 1st harmonic component is enough to achieve the original motion trend.

$$f(t) = a_0 + \sum_{j=1}^{n} \left\{ a_j \cos\left(j\frac{2\pi t}{T}\right) + b_j \sin\left(j\frac{2\pi t}{T}\right) \right\} \quad (4.1)$$

Where T is the wave encounter period and the coefficients a_0, a_j and b_j are given by;

$$a_0 = \frac{1}{T}\int_0^T f(t)dt \quad (4.2)$$

$$a_j = \frac{2}{T}\int_0^T f(t)\cos\left(j\frac{2\pi t}{T}\right)dt \quad (4.3)$$

$$b_j = \frac{2}{T}\int_0^T f(t)\sin\left(j\frac{2\pi t}{T}\right)dt \quad (4.4)$$

The results for 1st harmonic amplitudes and phases for heave and pitch motions are as shown in Figure 3 and Figure 4 respectively. From these figures, it can be seen that for the vertical ship motions, the 1st harmonic amplitudes increase linearly with increase in wave amplitude whereas the phases are fairly constant for all wavelength conditions.

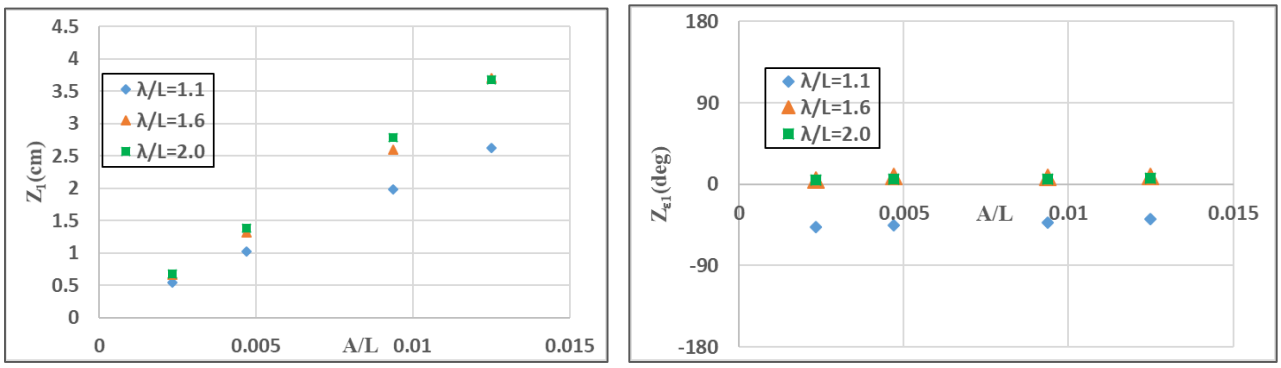

(a) (b)

Figure 3: (a) 1st Harmonic amplitudes and (b) phases for heave motion.

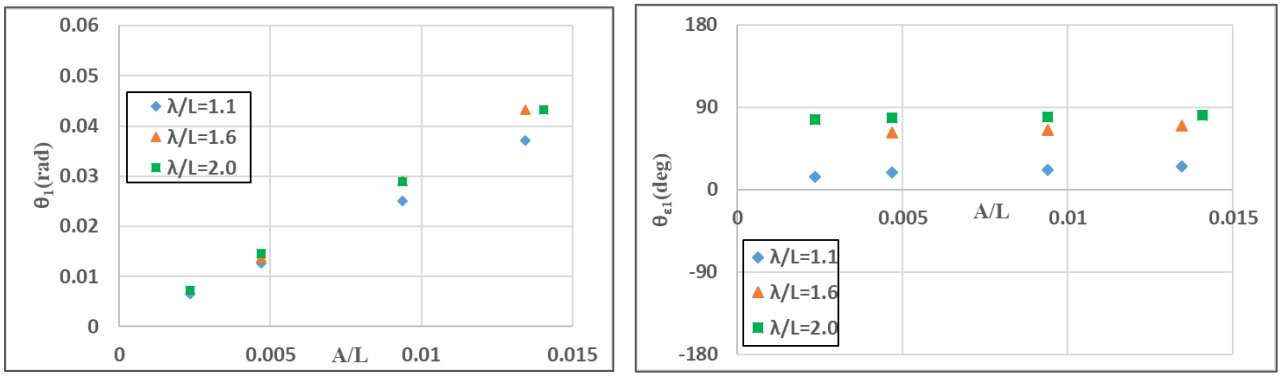

(a) (b)

Figure 4: (a) 1st Harmonic amplitudes and (b) phases for pitch motion.

For thrust, torque and effective wake, the mean values for λ/L=1.1, 1.6 and 2 are as shown in Table 2. These values are plotted against A/L (wave amplitude, A is non-dimensionalized by ship length, L) as shown in Figures 6(a), 7(a) and 8(a). From these figures and Table 2, it can be seen that the thrust and torque mean values decrease slightly whereas the effective wake mean values increase slightly with increase in the wave amplitude. The increase in effective wake mean values indicates an increase in the inflow velocity into the propeller plane which causes a slight decrease in the thrust and torque mean values.

The reconstructed thrust, torque and effective wake time histories for λ/L=1.1 are as shown in Figure 5. The shown wave amplitudes are measured values and not target values. In this paper, the result for λ/L=1.1

only is shown because the trends for thrust, torque and effective wake time histories for λ/L=1.6 and 2 are similar to those for λ/L=1.1.

Table 2: Mean values for thrust, torque and effective wake.

λ/L	A(cm)	Mean Values			
		Thrust(N)	Torque(N-m)	1-w	1-t
1.1	0.75	8.6285	0.1103	0.6434	0.8446
	1.5	8.5858	0.1096	0.6504	0.8433
	3	8.5809	0.1098	0.6508	0.8437
	4	8.5283	0.1093	0.6589	0.8443
	4.3	8.5235	0.1093	0.6596	0.8459
1.6	0.75	4.4556	0.0585	0.5899	0.8311
	1.5	4.4299	0.0586	0.5951	0.8337
	3	4.3733	0.0581	0.6060	0.8355
	4	4.3324	0.0584	0.6137	0.8378
	4.3	4.3110	0.0581	0.6180	0.8374
2	0.75	4.4403	0.0589	0.5930	0.8331
	1.5	4.4373	0.0593	0.5933	0.8350
	3	4.4080	0.0590	0.5984	0.8383
	4	4.3898	0.0585	0.6011	0.8361
	4.3	4.3657	0.0589	0.6056	0.8394

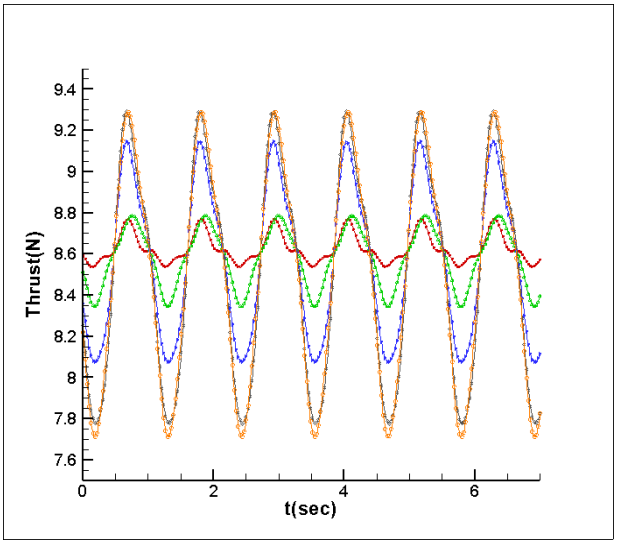

(a)

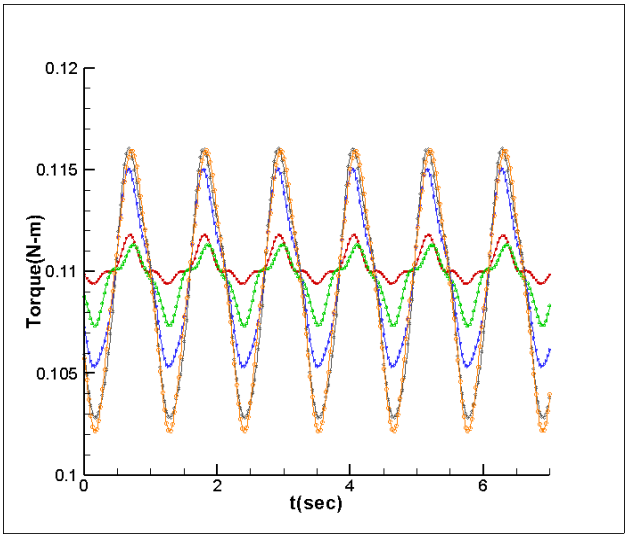

(b)

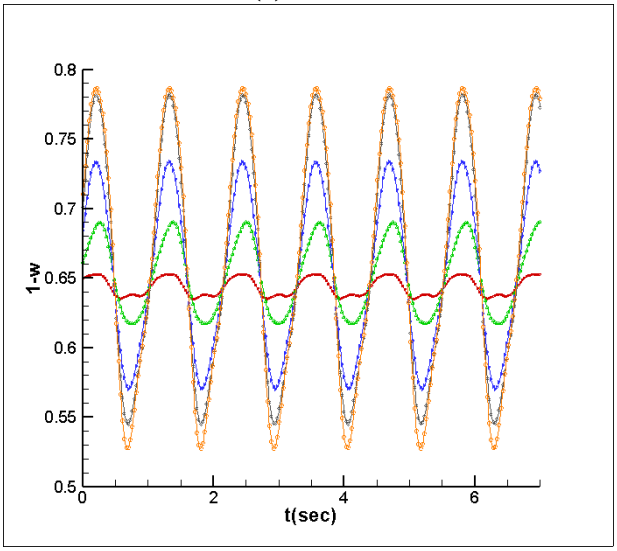

(c)

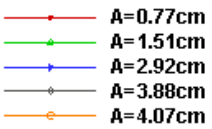

Figure 5: (a) Thrust, (b) torque and (c) effective wake reconstructed time histories at λ/L=1.1 for different wave amplitudes.

The effective wake and thrust deduction coefficients were calculated by equations 4.5 and 4.6 respectively;

$$1 - w = \frac{nJD}{V} \tag{4.5}$$

Where n is the propeller speed in revolutions per second, J is the propeller advance coefficient as obtained from the propeller open water chart and V is the ship speed.

$$1 - t = \frac{F_x - T - R_t}{T} \tag{4.6}$$

Where F_x is the x-force component in Newtons for with propeller condition, R_t is the resistance in Newtons in waves for without propeller condition and T is the propeller thrust in Newtons.

From Figure 5, it can be seen that the thrust and torque time histories are inverse to those of effective wake even though their amplitudes of oscillation increase with increase in wave amplitude. This explains the fact that the inflow velocity into the propeller plane influences the propeller thrust as will be discussed in section 4.2. Also, as the wave amplitude increases, the low thrust and torque regions increase downwards resulting in a slight decrease in their mean values, however, the high effective wake regions increase upwards resulting in a slight increase in its mean values.

The mean values and 1st harmonic values for thrust, torque and effective wake are as shown in Figure 6~8. It can be seen that the thrust and torque mean values decrease slightly while those for effective wake increase slightly as the wave amplitude increases. On the other hand, the 1st harmonic values for thrust, torque and effective wake increase linearly with increase in waves amplitude.

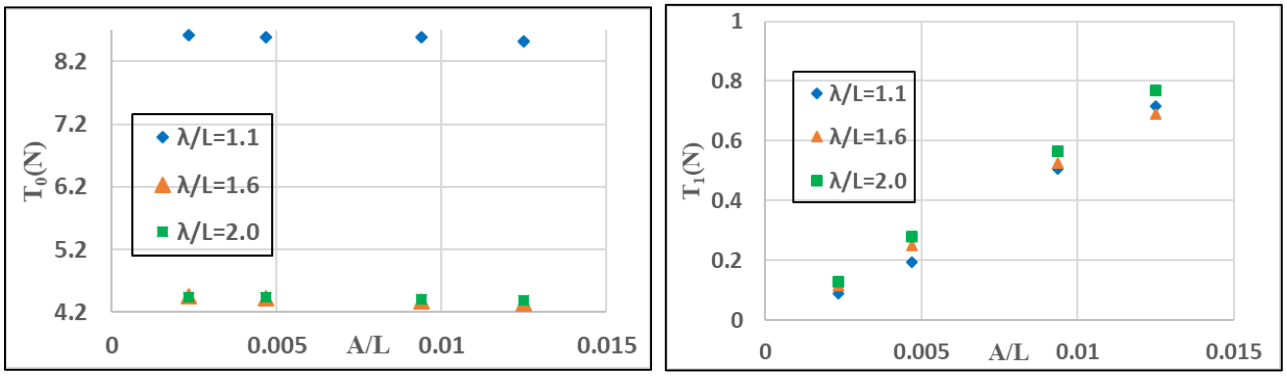

(a) (b)

Figure 6: (a) Mean values and (b) 1st harmonic values for thrust.

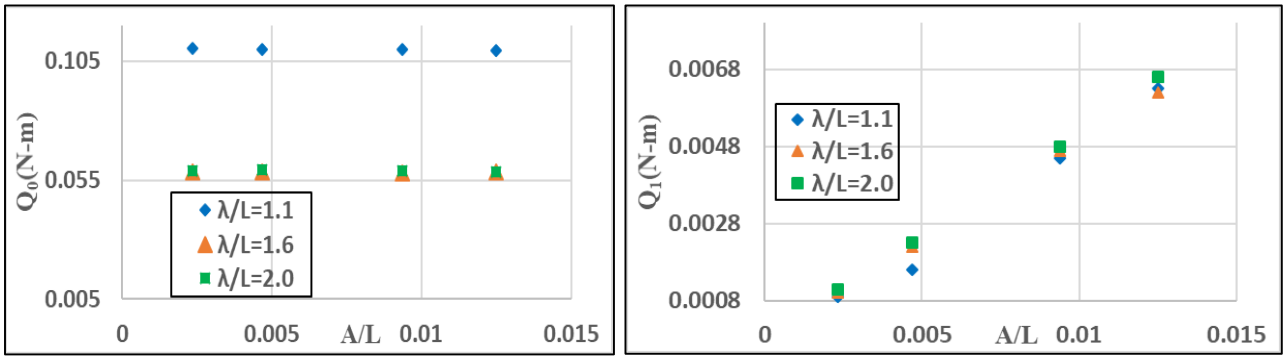

(a) (b)

Figure 7: (a) Mean values and (b) 1st harmonic values for torque.

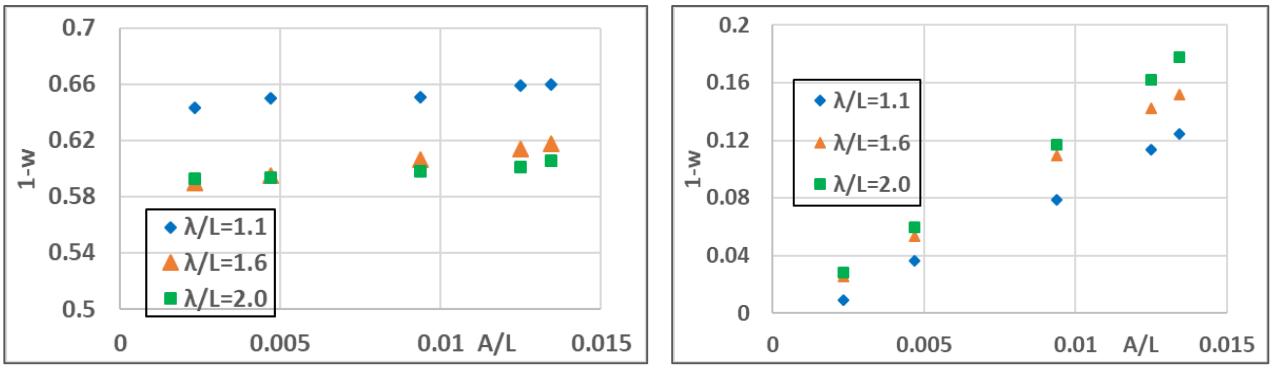

(a) (b)

Figure 8: (a) Mean values and (b) 1st harmonic values for effective wake.

4.2 SPIV Measurement Result

The PIV measurement was done for λ/L=1.1 and 1.6 at different wave amplitudes. The velocity field was phase averaged and the thrust fluctuation explained by this measured velocity field.

The phase-averaged velocity distribution diagrams for λ/L=1.1 are as shown in Figure 9~12 while those for λ/L=1.6 are as shown in Figure 13~15. From these phase-averaged velocity distribution diagrams, the vertical relative motion between the propeller disk and the low velocity region, due to bilge vortices, can clearly be seen, and sometimes the bilge vortices move outside the propeller radius. As the wave amplitude increases, this vertical relative motion increases and high velocity flow enters the propeller plane from the bottom. For λ/L=1.1, the inflow velocity into the propeller disk is highest at phase 90, when the ship stern is moving down, and lowest at phase 270, when the ship stern is moving up. This results in lowest propeller thrust at phase 90 and highest thrust at phase 270 as can be seen on Figure 16 (a). However, at λ/L=1.6 the inflow velocity into the propeller disk is highest at phase 270, when the ship stern is moving down, and lowest at phase 90, when the ship stern is moving up which results in lowest propeller thrust at phase 270 and highest thrust at phase 90 as shown in Figure 16 (b). Therefore, the inflow velocity into the propeller disk certainly influences the propeller performance such that when it is high, the propeller thrust is low and when it is low the propeller thrust is high.

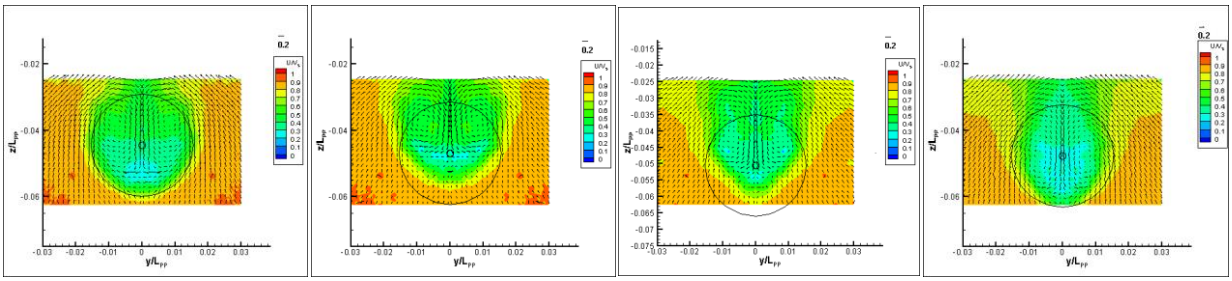

(a) 0 Degree (b) 90 Degree (c) 180 Degree (d) 270 Degree

Figure 9: Phase-averaged velocity distribution at AP for λ/L=1.1 and wave amplitude, A=0.75cm.

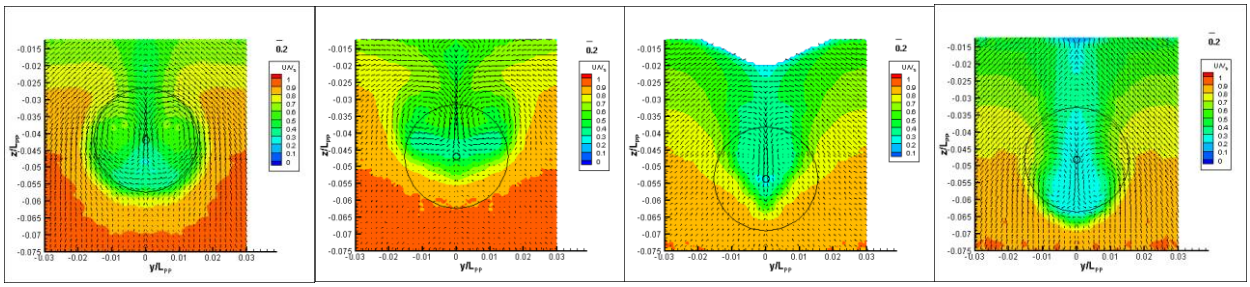

(a) 0 Degree (b) 90 Degree (c) 180 Degree (d) 270 Degree

Figure 10: Phase-averaged velocity distribution at AP for λ/L=1.1 and wave amplitude, A=1.5cm.

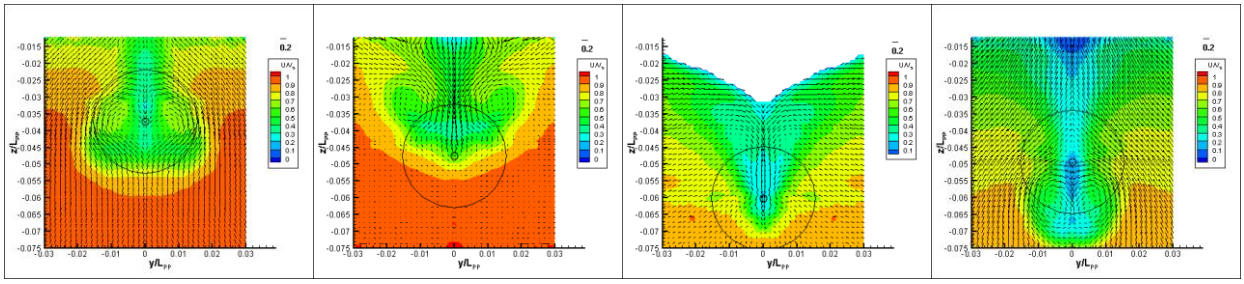

(a) 0 Degree (b) 90 Degree (c) 180 Degree (d) 270 Degree

Figure 11: Phase-averaged velocity distribution at AP for λ/L=1.1 and wave amplitude, A=3cm.

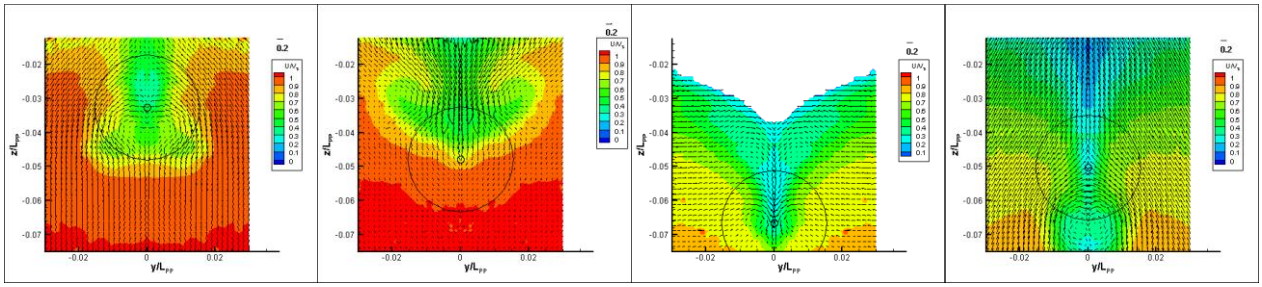

(a) 0 Degree (b) 90 Degree (c) 180 Degree (d) 270 Degree

Figure 12: Phase-averaged velocity distribution at AP for λ/L=1.1 and wave amplitude, A=4.3cm.

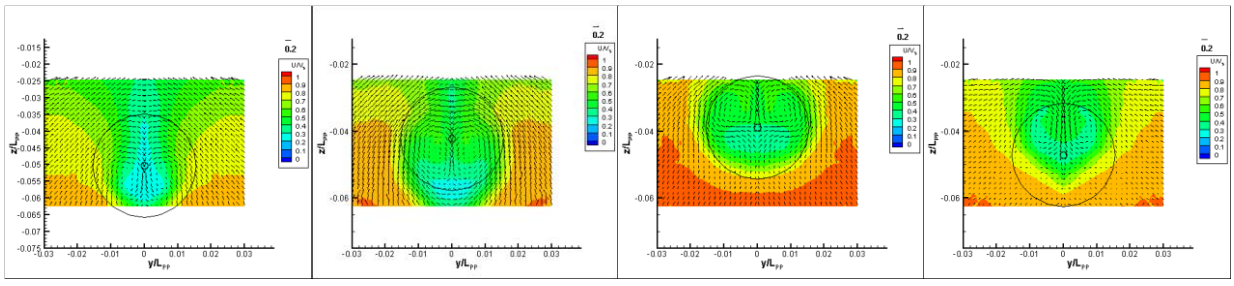

(a) 0 Degree (b) 90 Degree (c) 180 Degree (d) 270 Degree

Figure 13: Phase-averaged velocity distribution at AP for λ/L=1.6 and wave amplitude, A=1.5cm.

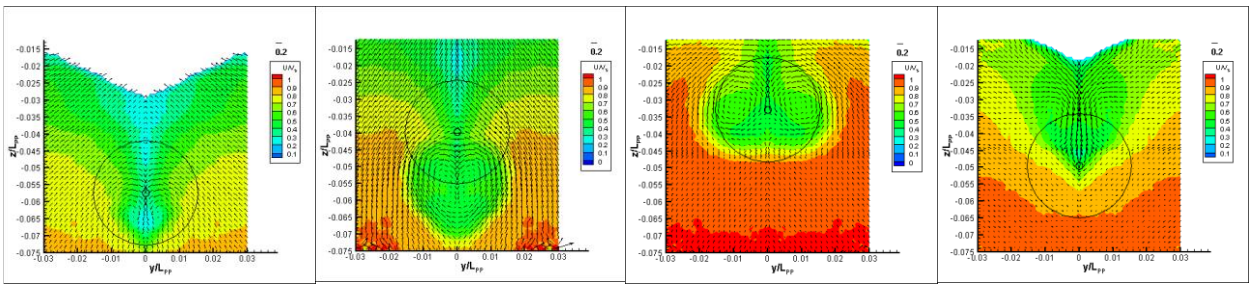

(a) 0 Degree (b) 90 Degree (c) 180 Degree (d) 270 Degree

Figure 14: Phase-averaged velocity distribution at AP for λ/L=1.6 and wave amplitude, A=3cm.

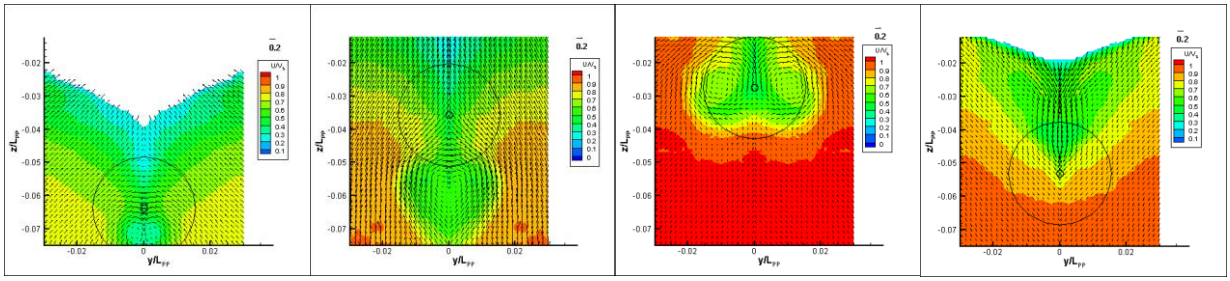

(a) 0 Degree (b) 90 Degree (c) 180 Degree (d) 270 Degree

Figure 15: Phase-averaged velocity distribution at AP for λ/L=1.6 and wave amplitude, A=4.3cm.

The velocity distribution was phase averaged at phases which are shown by the vertical lines on Figure 16. The true mean values for thrust are not zero as indicated in Figure 16, but the mean value has been intentionally subtracted from itself so as to have the thrust curve directly against the waves' curves in order to visualize how the thrust changes with the wave at the propeller. The wave peak is at the propeller plane.

5 CONCLUSIONS

The wave amplitude dependency for thrust, torque, towing force and 3DOF motion was investigated for KVLCC2 tanker model in long, regular head waves of different amplitudes at design Fr=0.142. The results were analysed by Fourier series expansion to determine the harmonic components responsible for original data trends and it was noted that for motions up to 1st harmonic was enough whereas for thrust and torque we need up to 3rd harmonic components to obtain the original trends.

The flow field around the ship stern was also measured by SPIV system and its change with the wave amplitude investigated. Moreover, the velocity distribution was analysed and discussed with respect to the thrust fluctuation in waves even though the velocity field was measured for without propeller condition. The vertical relative motion between the propeller disk and the low velocity region, due to the bilge vortices, was observed. As the wave amplitude increases this relative motion increases and high velocity flow enters the propeller plane from the bottom. This phenomenon certainly influences the propeller performance as explained in the results section.

Therefore, there is need to analyse this viscous inflow velocity into the propeller plane as an effort to improve the propulsive performance, including the engine characteristics, for ships in waves. This is one of the measures to reduce the GHG emissions from the shipping industry.

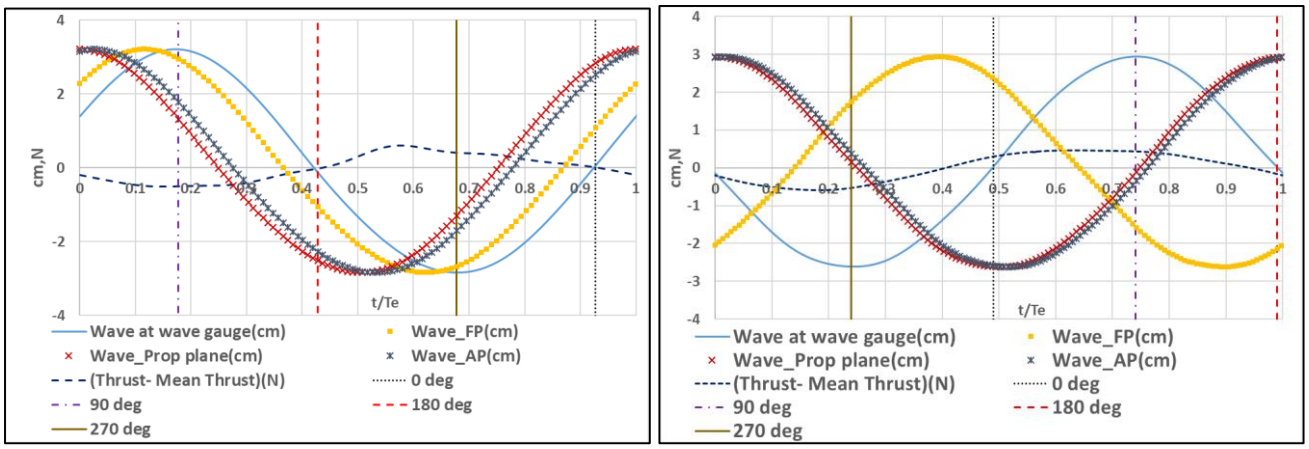

(a) (b)

Figure 16: Thrust and waves at various stations for one period at (a) λ/L=1.1 and (b) λ/L=1.6.

REFERENCES

[1] Nakamura, S. and Naito, S. "Propulsive performance of a container ship in waves". In: *Journal of the Society of Naval Architects of Japan*, 15 (1977), 24-48.

[2] Tsukada, Y., Hinatsu, M., and Hasegawa, J. "Measurement of unsteady ship wakes in waves". In: *Journal of Kansai Society of Naval Architects of Japan*, 228 (1997), 15-20.

[3] Calcagno, G., Di Felice, F., Felli, M. and Pereira, F. "Propeller wake analysis behind a ship by stereo PIV". In: *24th Symposium on Naval Hydrodynamics*, Fukuoka, Japan, 2002.

[4] Ohashi, K., Sakamoto, N. and Hino, T. "Numerical simulation of flows around KVLCC2 hull form with ship motions in regular waves". In: *International Conference on Computational Methods in Marine Engineering (MARINE)*, Hamburg, Germany, 2013.

[5] Sadat-Hosseini, H., Wu, P-C., Carrica, P.M., Kim, H., Toda, Y. and Stern, F. "CFD verification and validation of added resistance and motions of KVLCC2 with fixed and free surge in short and long head waves". In: *Journal of Ocean Engineering*, 59 (2013), 240-273.

[6] Wu, P-C. "A CFD study on added resistance, motions and phase averaged wake fields of full form ship model in head waves". *Doctoral Thesis*, Osaka University, Japan, 2013.

[7] Kim, H. "Phase-averaged SPIV wake field measurement for KVLCC2 plane propeller in waves". *Doctoral Thesis*, Osaka University, Japan, 2014.

[8] Wu, P-C., Okawa, H., Kim, H., Akamatsu, K., Sadat-Hosseini, H., Stern, F. and Toda, Y. "Added resistance and nominal wake in waves of KVLCC2 model ship in ballast condition". In: *Proceedings of the 30th Symposium of Naval Hydrodynamics*, Hobart, Tasmania, Australia, 2014.

[9] Tokgoz, E., Wu, P-C., Okawa, H., Tamaki, K. and Toda, Y. "Computation and SPIV measurement of the flow field around self-propelled ship in waves using body-force model". In: *Journal of the Japan Society of Naval Architects and Ocean Engineers*, 20 (2015), 255-258.

[10] Hossain, Md. A., Wu, P-C., Shibano, Y. and Toda, Y. "Forces, ship motions and velocity wake field for KRISO container ship model in regular head waves". In: *28th International Ocean and Polar Engineering Conference*, Sapporo, Japan, 2018.